The Effect of High Zeta Potentials on the Flow Hydrodynamics in Parallel-Plate Micro-Channels

A. Elazhary umelazha@cc.umanitoba.ca
Department of Mechanical and Manufacturing Engineering
University of Manitoba
Winnipeg, Manitoba, Canada R3T 5V6

H.M. Soliman hsolima@cc.umanitoba.ca
Department of Mechanical and Manufacturing Engineering
University of Manitoba
Winnipeg, Manitoba, Canada R3T 5V6

Abstract

This paper investigates the effect of the EDL at the solid-liquid interface on the liquid flow through a micro-channel formed by two parallel plates. The complete Poisson-Boltzmann equation (without the frequently used linear approximation) was solved analytically in order to determine the EDL field near the solid-liquid interface. The momentum equation was solved analytically taking into consideration the electrical body force resulting from the EDL field. Effects of the channel size and the strength of the zeta-potential on the electrostatic potential, the streaming potential, the velocity profile, the volume flow rate, the apparent viscosity, and the friction factor are presented and discussed. Results of the present analysis, which are based on the complete Poisson-Boltzmann equation, are compared with a simplified analysis that used a linear approximation of the Poisson-Boltzmann equation.

Keywords: Micro-fluidics, Fully developed, Laminar flow, Parallel-plate micro-channels, High zeta-potentials, Analytical solutions.

1. INTRODUCTION

Micro-scale fluid devices are increasingly becoming an attractive alternative to the conventional flow systems because of their compactness and large surface-to-volume ratio. These micro-scale devices are candidates for applications in heat transfer augmentation, micro-electronics and micro-electro-mechanical systems (MEMS), miniaturized chemical reactors and combustors, aerospace, and biomedical systems. Therefore, it is important to enhance our understanding of the relevant phenomena associated with fluid flow in micro-channels.

Due to the small sizes of these micro-channels, some surface phenomena (such as electrostatic forces and surface roughness) become significantly important. The present work is concerned with the effect of the electrostatic force associated with the electric double layer (EDL) on the fluid flow in micro-channels. Almost all solid surfaces have electrostatic charges, positive or negative, with different intensities. The fact that similar charges repel and different charges attract is the reason for the formation of the EDL. Consider a situation of negatively-charged surfaces

bounding a micro-channel carrying a pressure-driven liquid. The negative charges of the solid surface attract the positive charges in the liquid, while repelling the negative charges. As a result, an electric double layer (EDL) is created. The fluid flow under the influence of the pressure gradient pushes the charges in the diffuse layer towards the end of the channel giving rise to an electrical current called the streaming current. Consequently, the potential difference between the two ends of the channel generates an electrical current in the opposite flow direction known as the induction current. At steady-state conditions, a potential difference, namely the streaming potential, is generated between the two ends of the channel. The induction current carries charges and molecules in the opposite direction of the flow creating extra impedance to the flow motion which is called the electro-viscous effect. The maximum strength of the electrostatic charges occurs at the surface and is called the zeta-potential, ξ. The strength of the electrostatic potential, ψ, declines exponentially as we move away from the surface.

The existence of the EDL phenomenon has been known for over a century. Debye and Hückel [1] in 1923 linearized the exponential Boltzmann ion energy distribution and solved for the distribution of the electric potential in a solution at low wall potential. Their analysis, now known as the Debye-Hückel approximation, is valid only for situations where the zeta-potential is sufficiently low $(\xi \le 25\,\mathrm{mV})$. Later, Burgreen and Nakache [2] determined the ψ-distribution for electrokinetic flow in parallel-plate micro-channels at high ξ. The ψ-distribution was determined in terms of elliptic integral functions of the first kind. Mala et al. [3] used the Debye-Hückel approximation and solved analytically for the velocity distribution, volume flow rate, and friction factor during fully-developed laminar flow in a parallel-plate micro-channel. Li [4] extended the analysis to the geometry of two-dimensional rectangular channels. He determined the ψ-distribution, velocity distribution, and volume flow rate from an analytical linear solution (that used the Debye-Hückel approximation) and a numerical nonlinear solution (that used the complete Poisson-Boltzmann equation). Li noted large deviations between the two solutions, particularly in the region close to the channel walls. Chen et al. [5] investigated the fluid flow characteristics for developing, pressure-driven, liquid flow in parallel-plate micro-channels. The mathematical model (Poisson-Boltzmann, Nernst-Planck, continuity and Navier-Stokes equations) was solved numerically by means of a finite-volume method. For the micro-tubes geometry, Rice and Whitehead [6] solved for the fully-developed, laminar velocity distribution using the Debye-Hückel approximation and noted that, near the wall, the negative electrostatic force caused by the migration of ions can exceed the positive force due to the pressure gradient resulting in a region of back flow near the wall. Levine et al. [7] extended the work in [6] to conditions of high zeta-potentials. A review of the electro-kinetic effects on the flow hydrodynamics in micro-channels can be found in the recent book by Li [8].

The objective of the present investigation was to generate an analytical solution for the velocity distribution during steady, laminar, fully-developed flow of liquids in parallel-plate micro-channels using the full Poisson-Boltzmann equation. Therefore, the present analysis is expected to be valid for practical situations of high zeta-potentials. The results from the present analysis will be compared with the simplified solution (that uses the Debye-Hückel approximation) developed by Mala et al. [3] in order to assess of the effects of this approximation on the fluid-flow characteristics.

2. MATHEMATICAL FORMULATION

The geometry under consideration is shown schematically in Fig. 1, whereby a micro-channel is formed between two parallel plates separated by a distance 2*a*. An incompressible Newtonian aqueous 1-1 electrolyte of uniform dielectric constant ε flows in the micro-channel under the influences of an imposed pressure gradient dp/dz and a uniform zeta-potential x at both walls. A solution for the fluid-flow characteristics was obtained based on an analysis that is applicable to high x. The present analysis was conducted under the following assumptions:

1. The fluid is incompressible and Newtonian with constant thermo-physical properties.
2. The flow is considered to be steady, laminar, and fully developed.
3. The channel width (W) is much larger than channel height ($2a$), therefore, the flow is considered to be one-dimensional.
4. Non-slip conditions apply at both walls.

Electrostatic Potential Field

The electrostatic potential field (y) in the fluid region is governed by the Poisson–Boltzmann equation, which can be written as [3, 5]:

$$\frac{d^2\psi}{dx^2} = \frac{2 n_o z_v e}{\varepsilon \varepsilon_o} \sinh\left(\frac{z_v e \psi}{k_b T}\right). \tag{1}$$

The parameters n_o, z_v, e, ε_o, k_b, and T are the bulk concentration of ions, valence of ions, electron charge, permittivity of vacuum, Boltzmann constant, and absolute temperature, respectively.

Introducing the following dimensionless parameters:

$$\bar{\psi} = \frac{z_v e \psi}{k_b T}, \quad \bar{x} = \frac{x}{a}, \quad \text{and} \quad k = \left[\frac{2 n_o z_v^2 e^2}{\varepsilon \varepsilon_o k_b T}\right]^{\frac{1}{2}}, \tag{2}$$

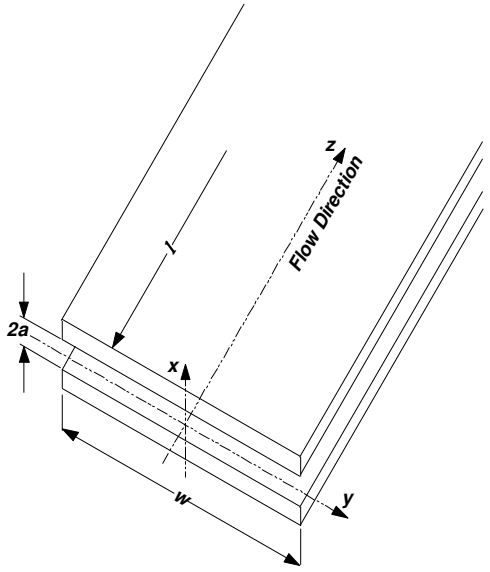

FIGURE 1: Geometry and Coordinate System

the dimensionless form of the Poisson–Boltzmann equation can be expressed as

$$\frac{d^2\bar{\psi}}{d\bar{x}^2} = (ka)^2 \sinh(\bar{\psi}). \tag{3}$$

The parameter k is the Debye–Hückel parameter and $(1/k)$ is normally referred to as the characteristic thickness of the EDL. Equation (3) is subject to the following boundary conditions:

$$\frac{d\bar{\psi}}{d\bar{x}} = 0 \quad \text{at} \quad \bar{x} = 0, \quad \text{and} \quad \bar{\psi} = \bar{\xi} \quad \text{at} \quad \bar{x} = 1, \tag{4}$$

where, $\bar{\xi} = \dfrac{z_v e \xi}{k_b T}$.

Integrating Eq. (3) and applying the boundary condition at the center of the channel, we get

$$\frac{d\bar{\psi}}{d\bar{x}} = \sqrt{2}(ka)\left[\cosh(\bar{\psi}) - \cosh(\bar{\psi}_o)\right]^{1/2}, \tag{5}$$

where $\bar{\psi}_o$ is the dimensionless electrostatic potential at the center of the channel. Assuming that the half-thickness of the channel is greater than the EDL thickness (i.e., $ka > 1$), we may set the parameter $\bar{\psi}_o$ in Eq. (5) to zero in order to facilitate the integration. The lowest value of ka used in the present analysis is 5.5. Integrating Eq. (5), apply the boundary condition at the channel wall, and rearranging, we get

$$\bar{\psi} = 4\tanh^{-1}\left[\tanh\left(\frac{\bar{\xi}}{4}\right)e^{-ka(1-\bar{x})}\right]. \tag{6}$$

The predicted $\bar{y}$ - $\bar{x}$ field from Eq. (6) as a function of (ka) and $\bar{x}$ will be compared with a numerical solution of Eq. (3) in order to confirm its validity.

Velocity Field

For steady, laminar, one-dimensional flow between parallel plates, the momentum equation (including the effect of EDL) has the following form:

$$\mu\frac{d^2v_z}{dx^2} - \frac{dp}{dz} + E_z\rho = 0, \tag{7}$$

where ρ is the charge density and it is defined as

$$\rho = -2(n_o z_v e)\sinh\left(\frac{z_v e\psi}{k_b T}\right), \tag{8}$$

and E_z is the electric field strength. The product $E_z r$ in Eq. (7) represents an electric body force and its effect appears to be the opposite of that of the pressure gradient. Utilizing the following dimensionless parameters:

$$G_1 = \frac{n_o k_b T}{L\left(-\frac{dp}{dz}\right)}, \quad \bar{v}_z = \frac{v_z}{v_o}, \quad \text{and} \quad \bar{E}_s = \frac{L E_z}{\xi}, \tag{9}$$

where v_o is a reference velocity given by $v_o = \frac{1}{\mu}\left(-\frac{dp}{dz}\right)a^2$, and substituting from Eq. (3), the momentum equation reduces to

$$\frac{d^2\bar{v}_z}{d\bar{x}^2} - \frac{2G_1\bar{\xi}\bar{E}_s}{(ka)^2}\frac{d^2\bar{\psi}}{d\bar{x}^2} + 1 = 0. \tag{10}$$

Equation (10) is subject to the following boundary conditions:

$$\frac{d\bar{\psi}}{d\bar{x}} = \frac{d\bar{v}_z}{d\bar{x}} = 0 \quad \text{at} \quad \bar{x} = 0, \quad \text{and} \quad \bar{\psi} = \bar{\xi} \quad \text{and} \quad \bar{v}_z = 0 \quad \text{at} \quad \bar{x} = 1 \tag{11}$$

Integrating Eq. (10) twice and imposing boundary conditions (11), the following velocity field was obtained:

$$\bar{v}_z = \frac{1}{2}\left(1 - \bar{x}^2\right) - \frac{2G_1\bar{\xi}^2\bar{E}_s}{(ka)^2}\left(1 - \frac{\bar{\psi}}{\bar{\xi}}\right), \tag{12}$$

where the electrostatic potential $\bar{y}$ is given by Eq. (6). The first term on the right-hand-side of Eq. (12) corresponds to the velocity component induced by the pressure gradient and the second term corresponds to the retardation due to the EDL. In order to calculate the velocity from Eq. (12), the streaming potential $\bar{E}_s$ must be determined.

Streaming Potential

The streaming current that is generated due to the transport of charges by the liquid flow can be calculated from the following integral:

$$I_s = \int_{A_c} v_z \rho dA_c. \tag{13}$$

Introducing the dimensionless parameters

$$\bar{\rho} = \frac{\rho}{n_o z_v e} = -2\sinh(\bar{\psi}) \quad \text{and} \quad \bar{I}_s = \frac{I_s}{2v_o n_o z_v e a}, \tag{14}$$

the streaming current equation can be written in the following dimensionless form:

$$\bar{I}_s = -2\int_0^1 \bar{v}_z \sinh(\bar{\psi})\, d\bar{x}. \tag{15}$$

Substituting from Eqs. (6) and (12) and performing the integration, the dimensionless steaming current can be written as

$$\overline{I}_s = I_1 - \left(\frac{4G_1\overline{\xi}\overline{E}_s}{(ka)^2}\right)I_2 - \left(1 - \frac{4G_1\overline{\xi}^2\overline{E}_s}{(ka)^2}\right)I_3 , \tag{16}$$

Where

$$I_1 = \frac{4}{(ka)^3}\left\{-ka\left[\ln\left(\frac{1+\eta e^{ka}}{1-\eta e^{ka}}\right) + \frac{\eta e^{ka}}{\left(\eta e^{ka}\right)^2 - 1}\right] + \left[\mathrm{Li}_2\left(\eta e^{ka}\right) - \mathrm{Li}_2\left(-\eta e^{ka}\right)\right] - \left[\mathrm{Li}_2(\eta) - \mathrm{Li}_2(-\eta)\right]\right\} \tag{17a}$$

$$I_2 = \frac{8}{ka}\left[\frac{1 - 2\eta e^{ka}\tanh^{-1}\left(\eta e^{ka}\right)}{\left(\eta e^{ka}\right)^2 - 1} - \frac{1 - 2\eta\tanh^{-1}(\eta)}{\eta^2 - 1}\right], \tag{17b}$$

$$I_3 = -\frac{4}{ka}\left[\frac{\eta e^{ka}}{\left(\eta e^{ka}\right)^2 - 1} - \frac{\eta}{\eta^2 - 1}\right], \tag{17c}$$

$$h = \tanh(\overline{x}/4)e^{-ka}, \tag{17d}$$

and $\mathrm{Li}_2(\beta)$ is the Poly-Logarithmic function of second order defined by

$$\mathrm{Li}_2(b) = -\int_0^b \frac{\ln(1-t)}{t}dt . \tag{17e}$$

An equilibrium state occurs when the streaming current is equal to the conduction current, i.e.,

$$I_c + I_s = 0 , \tag{18}$$

which can be written in the following dimensionless form:

$$\overline{I}_c + \left(\frac{G_2(ka)^2}{\overline{\xi}}\right)\overline{I}_s = 0 , \tag{19}$$

where $G_2 = \dfrac{L\varepsilon\varepsilon_o(-dp/dz)}{2\mu\lambda_o}$ and the dimensionless conduction current is $\overline{I}_c = \overline{E}_s\overline{A}_c/\overline{L}$. Substituting Eq. (16) into Eq. (19) and rearranging, we get

$$\overline{E}_s = \frac{\frac{G_2(ka)^2}{\overline{\xi}}(I_3 - I_1)}{1 - 4G_1G_2\left(I_2 - \overline{\xi}I_3\right)} . \tag{20}$$

Apparent Viscosity

The volume flow rate can be calculated from the relation

$$Q = 2W\int_0^a v_z dx\,. \tag{21}$$

In dimensionless form, Eq. (21) can be written as

$$\bar{Q} = \frac{Q}{2aW\,v_o} = \bar{v}_{zm}\,, \tag{22}$$

where the mean axial velocity, $\bar{v}_{zm}$, is given by

$$\bar{v}_{zm} = \int_0^1 \bar{v}_z d\bar{x} = \frac{1}{3} + \frac{4G_1\bar{\xi}\bar{E}_s}{(ka)^3}\left[\frac{(ka)\bar{\xi}}{2} + \left\{\mathrm{Li}_2\left(\eta e^{ka}\right) - \mathrm{Li}_2\left(-\eta e^{ka}\right)\right\} - \left\{\mathrm{Li}_2(\eta) - \mathrm{Li}_2(-\eta)\right\}\right]. \tag{23}$$

For poiseuille flow between two parallel plates without the EDL effect, the volumetric flow rate is expressed as

$$Q = \frac{2(-dp/dz)a^3W}{3\mu_a}\,, \tag{24}$$

where μ_a stands for the apparent viscosity. Equation (24) can be written as

$$\bar{Q} = \frac{\mu}{3\mu_a}\,. \tag{25}$$

Comparing Eqs. (22) and (25), we get after rearranging

$$\frac{\mu_a}{\mu} = \frac{1}{3\bar{v}_{zm}} = \frac{1}{3\bar{Q}}\,. \tag{26}$$

Friction Factor

The friction factor is normally defined as

$$f = \frac{2a(-dp/dx)}{\rho v_{zm}^2}\,, \tag{27}$$

and Reynolds number is given by

$$\mathrm{Re} = 4a\rho_f v_{zm}/\mu\,. \tag{28}$$

Combining Eqs. (27) and (28), and using the definition of G_1 given by Eq. (9), we get

$$f\,\mathrm{Re} = \frac{8}{\bar{v}_{zm}} = \frac{8}{\bar{Q}} \tag{29}$$

where $\bar{v}_{zm}$ is given by Eq. (23). Because μ/μ_a and $f\,\mathrm{Re}$ are directly proportional to $\bar{Q}$, as given by Eqs. (26) and (29), respectively, only the results of $\bar{Q}$ will be presented later.

3. RESULTS AND DISCUSSION

All the results presented in this paper correspond to an infinitely diluted aqueous 1:1 electrolyte solution ($n_o = 6.022 \times 10^{20}$ m^{-3}) at $T = 298$ K ($\varepsilon = 80$, $\lambda_o = 1.264 \times 10^{-7}$ Ω^{-1}m^{-1}, and $\mu = 0.9 \times 10^{-3}$ N s m^{-2}). A fixed pressure gradient $(-dp/dz) = 3$ atm/cm was used, while different values of a and ξ were utilized in generating the results. In the following figures, the results corresponding to the full model are based on the present analysis, while the results corresponding to the simplified model are based on the analysis of Mala et al. [3].

Figure 2 shows a comparison between three solutions of $\bar{\psi}$-distribution corresponding to $\xi = 240$ mv $\left(\bar{\xi} = 9.35\right)$ and $a = 1.7$ μm ($ka = 5.54$). The three solutions correspond to the full model given by Eq. (6), the simplified model of Mala et al. [3], and an accurate numerical solution of Eq. (3) together with boundary conditions (4). The close agreement between the full model and the numerical solution indicates that Eq. (6) produces accurate values of $\bar{\psi}$ throughout the channel at high zeta-potentials, thus confirming that the assumption of $\bar{\psi}_o = 0$ in Eq. (5) does not have a strong influence on the $\bar{\psi}$-distribution. On the other hand, the simplified model corresponding to the Debye–Hückel approximation deviates significantly from the other two sets of results.

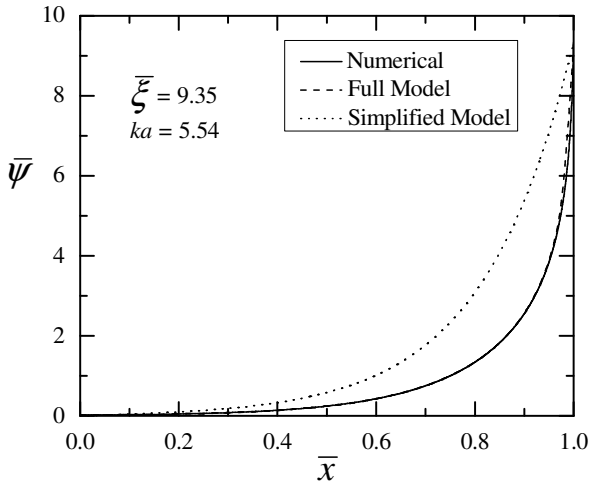

FIGURE 2: Validation of Eq. (6) for $\bar{\psi}$.

The influence of $\bar{\xi}$ on the $\bar{\psi}$-distribution at *ka* = 5.5 is shown in Fig. 3. Both the simplified and the full model predict that $\bar{\psi}$ increases with an increase in $\bar{\xi}$; however, the simplified model overestimates the value of $\bar{\psi}$ in all cases. Significant deviations can be seen between the two models at higher values of $\bar{\xi}$. It is clear from Fig. 3 that $\bar{\xi}$ is the key parameter in determining the magnitude of the deviation between the two models and that even for a narrow channel with *ka* = 5.5, the deviation can be small if $\bar{\xi}$ is small (e.g., $\bar{\xi} = 2$). The present result showing the simplified model over- predicting ψ at high ξ is consistent with previous results [4].

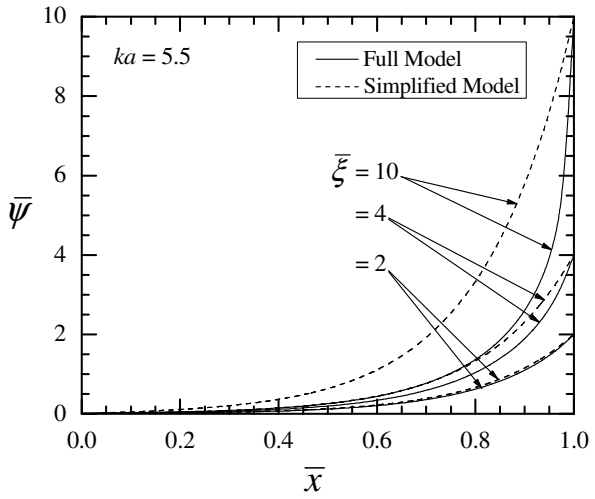

FIGURE 3: Effect of $\bar{\xi}$ on $\bar{\psi}$ at *ka* = 5.5.

Variation of the streaming potential, $\bar{E}_s$, with $\bar{\xi}$ and (*ka*) is shown in Fig. 4. Both the simplified and the full models predict that $\bar{E}_s$ decreases as $\bar{\xi}$ increases or (*ka*) decreases. An increase in ξ results in more ions being attracted in the double layer and less ions carried downstream by the flowing fluid and thus a lower E_s. Also, a decrease in (*ka*) decreases the volume between the plates resulting in less ions carried downstream and consequently a lower E_s. Figures 4 indicates that the simplified solution overestimates the value of $\bar{E}_s$ in all cases, consistent with the overestimation of $\bar{\psi}$ shown earlier. The deviation between the two solutions increases as $\bar{\xi}$ increases.

The velocity distributions predicted by both the simplified and the full models for the range $0 \le \bar{\xi} \le 10$ are shown in Fig. 5 for *ka* = 5.5. The profile marked $\bar{\xi}$ = 0 represents the velocity component induced by the pressure gradient without EDL retardation. Figure 5 shows that, as $\bar{\xi}$

increases, the full model predicts significant retardation of the flow velocity throughout the cross-section and a region of reversed flow near the wall up to $\bar{\xi}$ = 2. The deviation between the full model and the simplified model is insignificant at $\bar{\xi}$ = 0.5 and small at $\bar{\xi}$ = 2. Surprisingly, the magnitude of velocity retardation in the core region of the flow decreases as $\bar{\xi}$ increases from 2 to 10, while increased velocity retardation continues near the wall. As well, the near-wall zone (where increasing retardation continues) shrinks in size as $\bar{\xi}$ increases. This result is consistent with the near exponential decrease of $\bar{E}_s$ with $\bar{\xi}$, shown earlier in Fig. 4. It is important to note that the simplified model predicted an opposite trend in terms of the effect of $\bar{\xi}$ on the velocity retardation over the range 2 ≤ $\bar{\xi}$ ≤ 10. These results are consistent with those of Burgreen and Nakache [2] who reported that the retarding-flow component is less than 10% of the pressure-induced flow component for *ka* > 20, while for *ka* = 1.6, the retarding-flow component can be as much as 68% of pressure-induced flow component at $\bar{\xi}$ = 4. The results in [4] also indicate that for *ka* > 1, the magnitude of the retarding component decreased as $\bar{\xi}$ increased from 4 to 10.

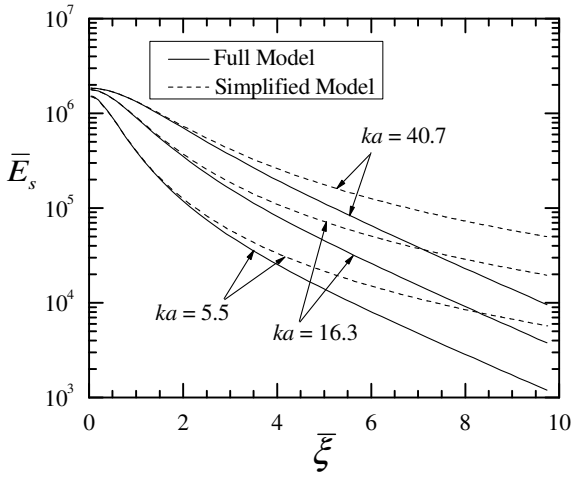

FIGURE 4: Variation of $\bar{E}_s$ with $\bar{\xi}$ and (*ka*).

Predictions of the dimensionless volume flow rate, $\bar{Q}$, are shown in Fig. 6. The full model predicts that $\bar{Q}$ decreases with $\bar{\xi}$ due to velocity retardation down to a minimum value at about $\bar{\xi} = 2.14$ for *ka* = 5.5 and about $\bar{\xi} = 3.31$ for *ka* = 40.7, and then increases with $\bar{\xi}$. The reduction in volume flow rate due to EDL is more significant for low values of *ka*; the maximum reduction is about 63% for *ka* = 5.5 and only about 9.6% for *ka* = 40.7. The trends in these results are consistent with the velocity results presented earlier. Values of μ_a/μ can be deduced from Fig. 6 using Eq. (26). As well, values of *f* Re can be deduced from Fig. 6 using Eq. (29).

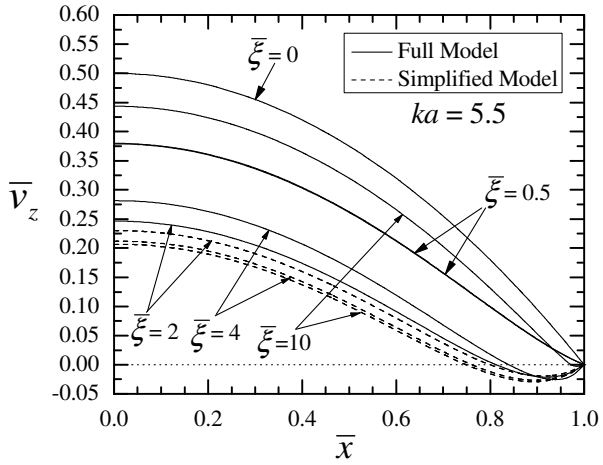

FIGURE 5: Velocity Profiles for ka = 5.5 and various $\bar{\xi}$.

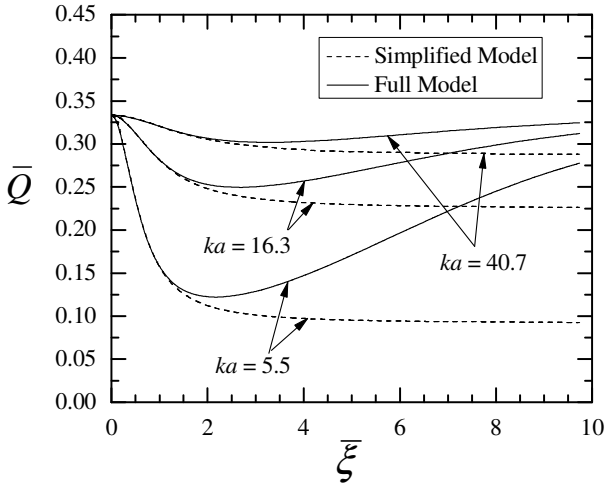

FIGURE 6: Variation of $\bar{Q}$ with $\bar{\xi}$ and (ka).

4. CONCLUSIONS

An analytical solution was developed for steady, laminar, fully-developed flow of liquids in a micro-channel formed by two parallel plates under the influence of an electric double layer (EDL). The solution was based on the full Poisson-Boltzmann equation and the results include the distribution of the electrostatic potential, ψ, the streaming potential, $\bar{E}_s$, the velocity distribution,

the volumetric flow rate, the apparent viscosity, and the friction factor. Comparisons were made between the predictions from the present (full) model and those from a simplified model based on the linearized Debye-Hückel approximation. The following conclusions can be drawn from the present results:

1. Both the simplified and the full models predict that $\bar{\psi}$ increases with an increase in $\bar{\xi}$ or a decrease in (*ka*); however, the simplified model overestimates the value of $\bar{\psi}$ in all cases. The deviations between the two models increase as $\bar{\xi}$ increases.

2. Both the simplified and the full models predict that $\bar{E}_s$ decreases as $\bar{\xi}$ increases or (*ka*) decreases. The simplified solution overestimates the value of $\bar{E}_s$ in all cases, consistent with the overestimation of $\bar{\psi}$, and the deviation between the two solutions increases as $\bar{\xi}$ increases.

3. The full model predicts that the magnitude of velocity retardation increases as $\bar{\xi}$ increases up to $\bar{\xi}$ = 2.14 (for *ka* = 5.5) and $\bar{\xi}$ = 3.31 (for *ka* = 40.7), beyond which the velocity retardation decreases with a further increase in $\bar{\xi}$. On the other hand, the simplified model predicts that the velocity retardation increases continuously as $\bar{\xi}$ increases.

4. The full model predicts that the volumetric flow rate decreases as $\bar{\xi}$ increases down to a minimum at $\bar{\xi}$ = 2.14 (for *ka* = 5.5) and $\bar{\xi}$ = 3.31 (for *ka* = 40.7), beyond which the volumetric flow rate increases with a further increase in $\bar{\xi}$. On the other hand, the simplified model predicts that the volumetric flow rate decreases continuously as $\bar{\xi}$ increases. The trends of the behaviours of the apparent viscosity and the friction factor follow the trend of the volumetric flow rate.

ACKNOWLEDGEMENT

The financial assistance provided by the Natural Sciences and Engineering Research Council of Canada (NSERC) is gratefully acknowledged.

5. REFERENCES

1. P. Debye, E. Hückel. “Zur theorie der elektrolyte. I. Gefrierpunktserniedrigung und verwandte erscheinungen“ Physik. Z., 24: 185-208, 1923

2. D. Burgreen, F.R. Nakache. “Electrokinetic flow in ultrafine capillary slits”. J. Physical Chemistry, 68: 1084-1091, 1964

3. G.M. Mala, D. Li, C. Werner, H.-J. Jacobasch, Y.B. Ning. “Flow characteristics of water through a microchannel between two parallel plates with electrokinetic effects”. Int. J. Heat Fluid Flow, 18: 489-496, 1997

4. D. Li. “Electro-viscous effects on pressure-driven liquid flow in microchannels”. Colloids and Surfaces, A: Physicochemical and Engineering Aspects, 195: 35-57, 2001

5. X.Y. Chen, K.C. Toh, J.C. Chai, C. Yang. “Developing pressure-driven liquid flow in microchannels under the electrokinetic effect”. Int. J. Eng. Sci., 42: 609-622, 2004

6. C.L. Rice, R. Whitehead. “Electrokinetic flow in a narrow cylindrical capillary”. J. Physical Chemistry, 69: 4017-4023, 1965

7. S. Levine, J.R. Marriott, G. Neale, N. Epstein. “Theory of electrokinetic flow in fine cylindrical capillaries at high zeta-potentials”. J. Colloid and Interface Science, 52: 136-149, 1975

8. D. Li. “Electrokinetics in Microfluidics”. Elsevier Academic Press, 2004.